Journal of Materials Chemistry C

HIGHLIGHT

View Article Online
View Journal | View Issue

A graphene-based transparent electrode for use in flexible optoelectronic devices

Cite this: J. Mater. Chem. C, 2014, 2, 2646

Kuldeep Rana, Jyoti Singh and Jong-Hyun Ahn*

Graphene, a monolayer of carbon atoms arranged in a honeycomb structure, is a unique material with outstanding properties that may be useful in applications ranging from electronic devices to energy storage devices. The versatile properties of graphene make it suitable for use in flexible and transparent optoelectronics, biological sensors, energy storage and conversion devices, electromechanical devices, and heat spreaders. This review focuses on recent progress in methods for graphene growth, modification, and transfer, and the uses of graphene as a transparent conducting electrode in flexible organic optoelectronic devices. Although prototypical laboratory-scale graphene-based devices have been prepared to demonstrate the advantages of graphene, many challenges must be addressed before such devices can be realized commercially.

Received 16th November 2013
Accepted 23rd January 2014

DOI: 10.1039/c3tc32264e

www.rsc.org/MaterialsC

1. Introduction

A new generation of flexible and stretchable devices has been extensively studied for use in electronics, optoelectronics, and energy harvesting applications. Such devices can maintain their original properties under high stresses and are designed to meet the anticipated demands of specific environmental conditions. Examples of such devices are flexible solar cells, displays, light-emitting diodes, flexible batteries, supercapacitors, heat spreaders, sensors, and detectors for use in biological applications. The key component needed for such devices is a flexible and stretchable electrode that can maintain its original electrical properties after bending or stretching under harsh environments. Thus, electrodes must be thin, lightweight, and highly elastic so that they can be stretched and flexed without compromising their conductivities and optical properties. Metallic nanowires,[1] carbon nanotubes (CNTs)[2–4] and conductive polymers[5,6] have been examined as potential transparent electrode materials; however, the surface roughness and uniformity of these materials degrades the performances of the final device and creates major drawbacks for their use as electrodes. Graphene has emerged as a good candidate material, as it displays most of the required characteristic features needed for electrodes in flexible devices.[7–9]

School of Electrical and Electronic Engineering, Yonsei University, Seoul, 120-749, Korea. E-mail: ahnj@yonsei.ac.kr

Kuldeep Rana received his M.S. degree in Physics from the HNBGU and PhD degree in Materials Engineering from the Indian Institute of Technology, Roorkee, India. He worked as a postdoctoral researcher in Bilkent University, Turkey, from 2010 to 2012. Currently he is working in the School of Electrical and Electronic Engineering, Yonsei University, Korea, as a postdoctoral researcher. His research focuses on the synthesis of graphene, carbon nanotube, AAO, and transition metal oxides for application in energy storage devices such as lithium ion batteries.

Jyoti obtained her BSc and MSc degrees from the University of Delhi, India. Afterwards she obtained her PhD degree in Materials Chemistry from the University of Delhi, India in 2012. Her PhD work included soft chemical synthesis of mixed metal oxides and their photocatalytic properties. She did her postdoctoral research at SungkyunKwan University and Yonsei University, South Korea under the supervision of Prof. J.-H. Ahn. Her research interests are chemical vapor deposition (CVD) and solution synthesis of graphene and molybdenum disulfide with a focus on their electrical properties.

Graphene is comprised of a monolayer of sp^2-hybridized carbon atoms, and is a semimetal in which charge carriers behave as Dirac fermions.[10] Graphene is thin, mechanically and thermally stable, impermeable to gases, optically transparent, chemically inert, and exhibits good electrical conductivity along with remarkable flexibility (elastic modulus $\approx$ 1 TPa).[11–15] The excellent flexibility of a graphene layer on a flexible substrate is advantageous: graphene flexible transparent conductors are yet to be characterized. The rich diversity of the physical and chemical properties of monolayer graphene has been examined in the context of a broad array of flexible devices, including field-effect transistors (FETs), organic light-emitting diodes (OLEDs), photosensors, and photovoltaics.[13,15–23] Having the smallest bending radius among all and despite the wide range of applications tested so far, several challenges remain before graphene may reach its full potential. For example a broader band gap would be needed before graphene could be used as a semiconductor material that could replace silicon in field-effect transistors.[9] Graphene doping has been explored in an effort to increase the carrier density and also use of high-k dielectric materials is always in demand.[24–26] The electrons in graphene behave as massless two-dimensional particles that may be described using the Dirac equation; hence, graphene displays a wavelength-independent absorption profile.[12] Monolayer graphene absorbs light between 400 nm and 6 μm through direct inter-band transitions, and the absorption intensity remains nearly flat throughout this spectrum. Monolayer graphene, therefore, is almost transparent and yields a transmittance exceeding 97%. Graphene displays a mobility of the order of 10^6, with a very high carrier concentration.[10] Good transparency and an excellent electrical conductivity render graphene as a promising candidate for use in a variety of optoelectronic devices. Transparent conducting films (TCFs) in electronic and optoelectronic devices are most commonly prepared using indium-tin-oxide (ITO).[27] When used as an electrode in an OPV cell, ITO exhibits a transparency of >90% and a sheet resistance of 10–30 Ω sq^{-1}; however, the brittle properties of ITO prohibit its use in next-generation flexible devices.[28] Other limitations of ITO-based electrodes are imposed by the materials' cost and chemical reactivity, which eventually degrade an organic device over time[29] and necessitates the replacement of the ITO electrode in the optoelectronic device. Graphene photodetectors have a wide spectral range and a high operating bandwidth (up to 40 GHz) compared to other semiconductor photodetectors.[30] Green OLEDs prepared from single-layer graphene transparent electrodes provide a current efficiency (CE) of $\gg$ 240 cd A^{-1} at a luminance of 20 000 cd m^2.[31] Flexible optoelectronic devices fabricated using graphene offer good performances and stable properties. Organic photovoltaics (OPVs) fabricated with CVD graphene have been shown to possess efficiency comparable to that of ITO devices and an outstanding capability while operating under bending conditions.[21]

This review focuses on methods for graphene synthesis, modification, and transfer to a target substrate. Recent progress in applications of graphene involving organic flexible optoelectronic devices, such as organic photovoltaics, organic light-emitting diodes (OLEDs), and photodetectors will be discussed. This article also reviews the importance and the merits of applications of graphene films as flexible transparent electrodes in optoelectronic devices.

Jong-Hyun Ahn obtained his PhD degree from POSTECH, Korea in 2001. From 2004 to 2008, he was a research associate at the University of Illinois at Urbana/Champaign; from 2008 to 2012 he worked at Sungkyunkwan University as an assistant/associate professor. Ahn currently holds post of the Underwood distinguished professor in the School of Electrical and Electronic Engineering at Yonsei University, Korea. His research interest focuses on the synthesis and properties of graphene and two-dimensional materials, and their application in flexible electronics. More details of the laboratory are available at http://graphene.yonsei.ac.kr

2. Graphene synthesis

The importance of graphene as a transparent conducting electrode for use in various electronic and optoelectronic devices stems from the extraordinary properties of graphene. The synthesis of high-quality graphene with these characteristic features is an important issue. A variety of methods may be used to synthesize graphene and transfer it to flexible or rigid substrates prior to use in devices. The first method developed for the production of graphene involves the micromechanical exfoliation of graphite.[32] This method yielded high-quality graphene; however, the yield was low, the process was unsuitable for industrial applications, and the uses of this graphene were limited to fundamental studies. The most promising large-area inexpensive approach to prepare reasonably high-quality graphene involves chemical vapor deposition (CVD) through decomposing methane or ethylene on a transition metal surface, such as palladium, copper, or nickel.[33–35] Recently, uniform high-quality large-area graphene has been grown on copper surfaces at low temperatures to provide a very high mobility of up to 7350 cm^2 V^{-1} s^{-1}.[7] Hydrocarbons decompose at a Cu or Ni surface, and the resulting carbon atoms dissolve into the surface to form a solid solution. Ni displays a relatively high carbon solubility (of 2.7 at%) compared to Cu (0.04 at%) at higher temperatures, and the carbon solubility decreases as the temperature decreases.[36] After rapid cooling, the carbon atoms diffused on the surface through a segregation and precipitation mechanism to form mono- or few-layer graphene, depending on the cooling rate.[37–39] Different growth mechanisms have been proposed to describe the graphene growth process. Ni segregation may contribute to graphene growth in some contexts. By contrast, Cu offers a very low carbon solubility (see Fig. 1a). After the formation of the first carbon layer, Cu does not induce further hydrocarbon decomposition. The deposition process,

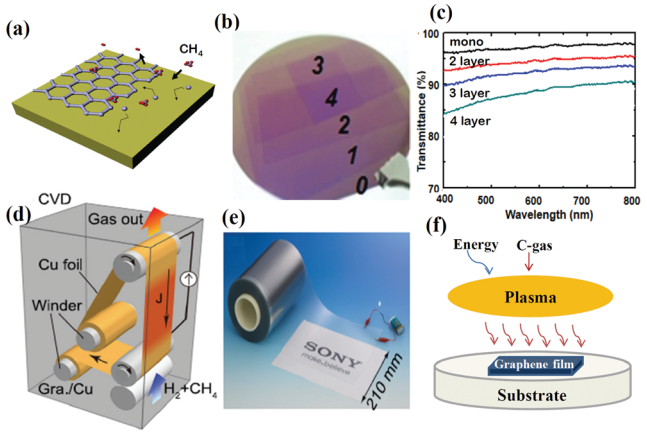

Fig. 1 (a) Schematic diagrams of the graphene growth mechanism on Cu, (b) optical images of graphene transferred to SiO_2/Si substrates from the Cu substrate, (c) optical transmittance of different layers of graphene, (d) a continuous roll-to-roll CVD system using selective Joule heating to heat a copper foil suspended between two current-feeding electrode rollers to 1000 °C to grow graphene, (e) photograph of the graphene plastic roll before the widths of the graphene/epoxy and base PET films are 210 mm and 230 mm, respectively and (f) schematic illustration of the plasma CVD method. Reprinted with permission from ref. 41. Copyright 2013 American Institute of Physics.

therefore, forms monolayer graphene.[39,40] The optical transmittance gradually decreases by about 2.3% according to the number of stacked graphene layers (Fig. 1b and c). Recently, high-quality graphene with a sheet resistance of 150 Ω sq^{-1} and a length of 100 m was fabricated *via* a roll-to-roll CVD method on a copper foil, followed by a transfer step.[41] Fig. 1d shows the design of the roll-to-roll CVD system prepared using a stainless steel vacuum chamber and a copper foil heated to 1000 °C under Joule heating. The deposition reaction proceeded for more than 16 h. Graphene films have been printed on a polyethylene terephthalate (PET) transparent film with a length of 100 m (Fig. 1e). In addition, recently researchers made an effort to develop low temperature synthesis methods using plasma CVD techniques such as microwave, surface wave, and inductively coupled plasma (Fig. 1f).[42–45] These plasma CVD methods are a promising route for growing graphene at lower substrate temperatures. During the thermal CVD process, the carbon source dissociates at a high temperature, whereas during plasma CVD, carbon fragments in the form of C_2 radicals are generated around 300–500 °C. The polycrystalline Cu and Ni films used to grow graphene during plasma CVD over very short times have revealed that a direct growth mechanism plays an important role in this process.

A solution-method based on an oxidation and reduction process is another important method for producing graphene, which is cost-effective on high-volume production scales. The earliest reports on synthesis of graphene oxide (GO) trace back to Brodie's work using concentrated acids in the presence of an oxidizing agent.[46] Each oxidized flake has a large number of negative charges and repels one another. A similar method has been used recently to produce almost single layer GO, which has a thickness of approximately 1–1.4 nm.[47,48] The resulting GO can be reduced partially by various methods such as the chemical method,[49] annealing in an NH_3 atmosphere[50] or by laser irradiation.[51,52] The reduction process depends on the number of methods and parameters used. The properties of GO and reduced graphene oxide (rGO) can be tuned by film thickness, chemical modification, flake size and morphology. As synthesized GO films are typically insulating, they generally show a high sheet resistance of 10^{12} Ω sq^{-1},[13] which is attributed to the absence of an electronic pathway in the basal plane. However, annealed rGO shows the sheet resistance of 10^2–10^3 Ω sq^{-1} [53] and an electrical conductivity of ~7200 S m^{-1}.[47] Similarly reported by other researchers[54–57] the high-yield and low-cost chemical route to graphene synthesis is important for industrial applications; however, the graphene produced by the solution process includes a significant quantity of impurities, oxygen atoms, and defects. These features can be removed by thermal annealing to improve the purity and uniformity of the electronic structure.

Graphene produced by the methods described above does not provide good conductivity values suitable for practical applications as transparent conductive electrodes. The electrical properties of graphene may be improved by using a variety of strategies. Graphene films comprising a few layers are the most valuable to the research and industrial communities. The electrical properties of graphene are closely related to its thickness. Bilayer graphene offers a tunable band gap that is not present in monolayer graphene, the stacking order and coupling between graphene layers can affect the electrical properties.[58] Together with the band gap opening properties of graphene, the type of charge carrier is a key consideration for any device application. The conductivity of graphene and the type of carrier can be modified using chemical doping or electrostatic doping. The sheet resistance and transmittance of pure and doped graphene have been summarized in Table 1. Nitric acid acts as a p-type dopant that accepts electrons from graphene and reduces the sheet resistance to 150 Ω sq^{-1}.[33] Similarly, polyvinyl alcohol (PVA) induces n-type doping with a sheet resistance value that decreases from 4 kΩ sq^{-1} to 400 Ω sq^{-1} without affecting the transmittance.[11] Chemical doping approaches suffer from problems with sheet resistance degradation over time due to the adsorption of moisture, thereby limiting the practical applications of chemically doped graphene. Recently, Yan *et al.* reported a method of protecting chemically doped graphene by applying a coating of a curable polymer (poly(4-vinylpyridine)) with a proven capacity to preserve the conductivity of a doped graphene film under ambient conditions over periods exceeding 2.5 months.[59] The sheet resistance degradation over time in chemically doped graphene can be improved by introducing non-volatile doping effects. Ferroelectric polarization of the piezoelectric material, such as poly(vinylidene fluoride-*co*-trifluoroethylene) (P(VDF-TrFE)), can effectively enhance the conductivity of graphene and preserve its properties over long times.[60] The sheet resistance can be reduced to 120 Ω sq^{-1}, and a high optical transparency and mechanical flexibility may be provided, all of which properties are critical for applications in graphene-based optoelectronics.

Table 1 Sheet resistance and optical transmittance of a graphene thin film

Graphene film	Sheet resistance (Ω sq^{-1})	Transmittance (wavelength in nm)	Ref.
CVD-graphene(G) on Ni	280	76% (550)	33
CVD-G on Cu	350	90% (550)	61
CVD-G doped with HNO_3	30	90% (550)	7
CVD-G doped with $AuCl_3$	150	87% (550)	62
CVD-G doped with polyvinyl alcohol	400	98% (550)	11
CVD-G with electrostatic doping by p(VDF-TrFE)	120	95% (550)	60
Spin coated rGO	10^2–10^3	80% (500)	63
Electrochemically exfoliated	2.4×10^3	73%	54
Vacuum filtrated rGO	4.3×10^4	73% (550)	13
LB-rGO	1.9×10^7	95.5% (650)	64
LB-chemically modified G	8×10^3	83% (1000)	65
LB-rGO	1100	91% (550)	66
CVD-G/GO	—	88% (550)	67

3. Transfer of graphene films

The previous section described various methods that have been developed for growing large-area high-quality graphene. The next critical step toward a study of the fundamental properties and practical applications of graphene involves the transfer of graphene from a metal substrate to a desired target substrate without undermining the quality of the graphene. Poly(methyl methacrylate) (PMMA) is the most common graphene support substrate used to transfer graphene onto other substrates.[40] Graphene films transferred using this method tend to retain a PMMA residue on the graphene surface that then induces tearing in the graphene surface after rinsing. Recent roll-to-roll methods rely on the use of a thermal release tape for graphene transfer. This technique is readily scaled up to large-area graphene transfer processes; however, the thermal release tape affects the resulting device performance.[7] CVD graphene may become contaminated by the presence of oxidized metal particles that form during chemical etching processes which, after the transfer step, become trapped at the interface between graphene and the substrate. The trapped contaminants act as carrier transport scattering centers and degrade the device performance. Another important issue associated with graphene transfer involves crack formation and the tearing of graphene. Current graphene transfer techniques, therefore, present significant challenges. A "modified RCA clean" transfer method was recently introduced in an effort to control the contamination and avoid degradation. This method yields good-quality graphene films after transfer[68] and involves an effective metal cleaning process in which the hydrophobicity of the target substrate is controlled. The electrical properties of the transferred graphene do not degrade significantly, and high device yields of up to 97% have been achieved. Song *et al.* described an important method that enabled high-fidelity graphene transfer onto a variety of surfaces, including a fragile polymer, a thin film, or a hydrophobic surface.[69] In this method, a 'self-release layer' (SRL) was inserted between the elastomer and the graphene film. Transfer to the stamp provided a mechanical support that avoided bending stresses that caused the graphene film to fracture. The stamp with a graphene face was brought in contact with the target substrate, and the assembly was baked at 100–120 °C for 1–3 min to achieve conformal contact and adhesion. A subsequent lift-off process left the graphene on the target substrate. The low adhesive force between the stamp and the release polymer, as compared to the graphene and the target substrate, favored dry transfer. Transfer processes that involve harmful chemical etchants used for etching a metal substrate can damage the graphene layer. Lock *et al.* demonstrated the use of an azide-based linker molecule for CVD graphene exfoliation transfer (Fig. 2a). The linker molecules were deposited on the polystyrene substrate, and graphene was subsequently attached to the linker molecules. By applying heat and pressure, the linker molecules formed strong covalent bonds that assisted the clean transfer of graphene from the catalyst metal.[70] A similar method was developed by Yoon *et al.*, in which a thin layer of epoxy was used to peel away the graphene. During the peeling process, the measured adhesion energy between graphene and Cu (0.72 ± 0.07 J m^{-2}) was found to exceed the adhesion energy between graphene and silicon (0.45 ± 0.02 J m^{-2}).[71] Recently, a unique technique involving a "clean-lifting transfer (CLT)" method was developed

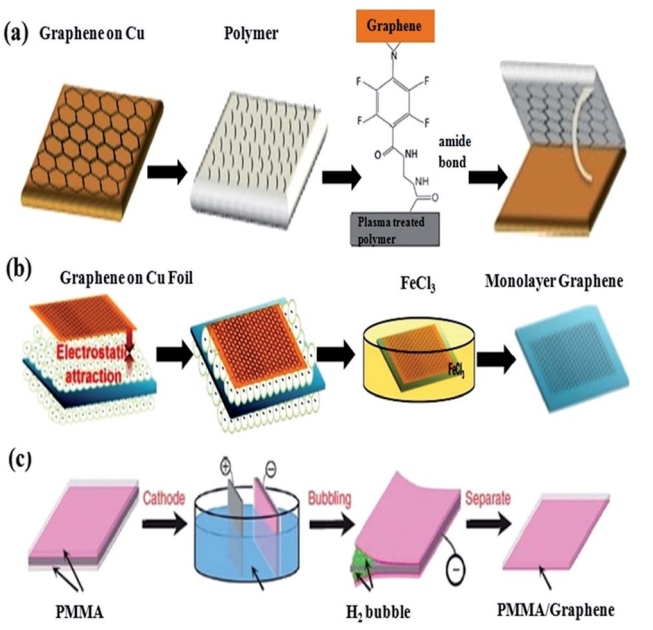

Fig. 2 Different processes of graphene transfer (a) flow chart of graphene transfer using the treated polymer and transferred to a flexible substrate. (b) Schematic illustrations of the CLT processes of as-grown graphene on a Cu foil onto a flexible PET substrate. (c) Illustration of the bubbling transfer process of graphene from a Pt substrate. Reprinted with permission from ref. 70. Copyright 2011 American Chemical Society, ref. 72. Copyright 2013 WILEY-VCH Verlag GmbH & Co. KGaA, Weinheim and ref. 73. Copyright 2012 Macmillan Publishers Limited.

in which an electrostatic force was harnessed to avoid the need for an organic support. This method is highly scalable for production, low-cost, time-efficient, and useful for the production of high-quality large-area graphene-based devices for industrial applications.[72] Fig. 2b shows a schematic diagram of the CLT process, which was applied to the transfer of CVD graphene onto an arbitrary substrate. Charge was first accumulated on a target substrate. The graphene surface of the Cu foil was then attracted to the substrate under the electrostatic force. Pressing the substrate created a uniform distribution of attachment points between the graphene and the substrate. The Cu foil was then etched away using an iron nitrate solution, followed by rinsing in de-ionized water to remove any residue. The large-area graphene films were transferred onto a flexible polyethylene terephthalate (PET) surface. Graphene transfer using the CLT technique has significant potential for future industrial applications of flexible graphene-based electronics and optoelectronics. A bubbling method is also reported to transfer millimetre-sized hexagonal single-crystal graphene and graphene films by Gao *et al.* In this method, a Pt/Graphene/PMMA structure was used as the cathode in an electrolysis cell wherein at the cathode, water reduction produced H_2 gas and the bubbles arising out of this detached the graphene from Pt within seconds (Fig. 2c). The transfer is non-destructive and the transferred graphene has the lowest reported wrinkle height of 0.8 nm.[73]

In a similar way to the CVD graphene, GO and rGO are required to be printed on a flexible, bendable and transparent substrate for use as a transparent and conducting electrode in various flexible optoelectronic devices. By taking advantages of their volume production at low cost and tunable electrical and optical properties, GO and rGO thin films can be used for a number of applications. The GO and rGO films can be formed on diverse substrates by using various techniques such as drop and dip casting,[74,53] spin coating,[69,15] Langmuir–Blodgett (L–B)[72,75] and vacuum filtration.[76] Different methods have their respective advantages or disadvantages – *e.g.* the dip and drop casting result in uneven deposition, and the van der Waals forces keep the GO film bound to substrate.[87] Use of the vacuum filtration method produces reasonably good nanometer thick films which can be transferred onto various substrates by gently pressing the films. This method successfully demonstrated fabrication of a GO film, single-walled carbon nanotubes (SWNTs) and free standing paper[77] for transparent and flexible devices[78]. The highly uniform and closed packed film of GO can be formed by the L–B method.[64] Recently, an ultra large GO film with a controlled structure has been produced on a PET substrate using the L–B method.[79,80] This method permits the deposition of GO films onto any arbitrary substrate in different sizes depending on the LB vessel. Spin coating is a more convenient method for preparing transparent conductive films *e.g.* in the case of a solar cell where high transmittance and low resistance multilayer graphene are required. Spin coated films are highly continuous which cover the entire surface of the substrate, and the thickness of the graphene film can be controlled easily by monitoring the coating speed and GO concentration.[15]

4. Flexible optoelectronic device applications

After transferring the large-area residue-free graphene film onto a target substrate, the graphene may be used as a transparent conducting electrode in a variety of flexible devices, such as OPVs, OLEDs, and photodetectors (Table 2).[81–83] An ideal electrode with a high optical transparency, low sheet resistance, and appropriate work function is an essential part of an optoelectronic device. The device fabrication costs are also important for commercialization. Most devices in this field are prepared using indium tin oxide (ITO) as a transparent conducting electrode which has a number of disadvantages as discussed above and limit the applicability in flexible devices. The development of new transparent conducting and flexible electrodes for use in flexible optoelectronic devices would be highly desirable. Graphene is a good candidate material for replacing ITO electrodes due to its outstanding electrical and mechanical properties.

4.1 Organic photovoltaics

Several groups have attempted to use graphene as a transparent conductive and flexible electrode in OPVs.[84–86] Graphene can also be used as a photovoltaic active layer[87] or an electron transport bridge.[88] Solution-processed rGO, when used as a transparent electrode in an OPV, provided a low power conversion efficiency (PCE) of 0.13% due to the high sheet resistance (17.9 kΩ sq^{-1}) and hydrophobic nature of the graphene.[89] Further improvements in the PCE of a flexible OPV prepared using rGO have been obtained by lowering the sheet resistance or modifying the work function using a graphene/CNT composite.[90] Laser-reduced GO (LrGO) techniques[91] have been introduced in an effort to increase the PCE to 1.27% in flexible OPVs. CVD has emerged as an important method for the growth of high-quality, large-area graphene films with relatively good sheet resistance and optical transparency. Such a method has accelerated the practical applications of graphene as transparent electrodes in OPVs. Recent reports have described the fabrication of flexible OPVs using a plastic substrate, highly doped multilayer CVD graphene as the anode, and P3HT:PCBM as the active layer.[92,93] The thin and extremely flexible OPVs provided a maximum PCE of 3.2% with excellent bending stability. Fig. 3a displays the *J–V* characteristics of OPVs prepared using different numbers of graphene layer electrodes. The two-layer graphene electrode exhibited the best performance, with a PCE of 3.17%. Fig. 3b shows the structure of a flexible OPV prepared using CVD graphene. The bending stability of the OPV prepared using a two-layer graphene electrode was measured up to a bending radius of 3 mm. The PCE was 8% lower than the original value after 1000 bending cycles. The series resistance of the two-layer graphene electrode OPV was 7% higher than the original value after 1000 cycles of bending, whereas the series resistance of the monolayer graphene OPV was 16% higher after the same experiment. The degradation of the OPV during bending was attributed to the change in the graphene electrode morphology and the active layer of the device. The

Table 2 Various optoelectronic devices based on graphene (rGO, CVD-G) electrodes

Device	Graphene type	Sheet resistance	T (%)	PCE (%)	Ref.
OPV	rGO	1 kΩ sq^{-1}	80	1.01	76
	rGO	17.9 kΩ sq^{-1}	85–95	0.13	89
	rGO-CNT	240 kΩ sq^{-1}	86	0.85	90
	LrGO	700 Ω sq^{-1}	44	1.1	91
	CVD-G doped with PEDOT:PSS	350 Ω sq^{-1}	88	2.7	84
	CVD-G doped with PEDOT:PSS and Au	158 ± 30 Ω sq^{-1}	90	3.2	92
	CVD-G doped with $SOCl_2$	450 Ω sq^{-1}	90	2.5	93
	CVD-G doped with HNO_3	36.6 Ω sq^{-1}	85	4.33	94

	Graphene type	Doping	Substrate	PCE (%)	Ref.
DSSC	CVD-G	Fluorine	Fluorine-doped tin oxide	2.56	95
	rGO nanosheet	—	Fluorine-doped tin oxide	6.81	96
	CNT/rGO	—	Graphite	6.17	102
	CVD-G	—	Graphene paper	6.05	77
	PEDOT/CVD-G	HNO_3	PET	6.26	85

Device	Graphene type	Doping	Emission type	Luminous eff. (lm W^{-1})	Ref.
OLED	rGO	—	Fluorescent	0.35	99
	rGO	p-Doping	—	5	100
	CVD-G	—	Phosphorescent	0.53	103
	CVD-G	HNO_3	Fluorescent	37.2	101
	CVD-G	HNO_3	Phosphorescent	102.7	101
	CVD-G	Triethyloxonium hexachloroantimonate	Phosphorescent	80	31

	Graphene type	Devices	Photoresponsivity	Ref.
Photo detector	rGO	P3HT with RGO on PET	5 mW cm^{-2}	110
	Mechanically exfoliated G	Monolayer G	8.61 A W^{-1}	105
	Mechanically exfoliated G	G nanoribbons (GNRs)	1 A W^{-1} (at 1550 nm)	111
	CVD-G	G/gold nanostructure	2.2 mA W^{-1}	104
	CVD-G	PbS QDs/G/flexible substrate	10^7 A W^{-1}	77
	CVD-G	ZnO nanoparticle–G core–shell structure	640 A W^{-1}	107

package-free flexible OPV prepared using a two-layer graphene electrode protected the OPV components from contamination. Fig. 3c shows the current density *versus* voltage characteristics of CVD graphene flexible photovoltaic cells which provide a maximum PCE of 1.18% in the bending state. This PCE can be compared favorably to the PCE obtained from an OPV prepared using an ITO electrode in the same cell structure (1.27%).[21] These results indicated that graphene functioned well as a transparent conducting electrode in a flexible OPV, particularly air-sensitive devices. In addition, H. Kim *et al.*, recently demonstrated a highly efficient, flexible OPV device with a PCDTBT:PC70BM active layer that displays a quite good value of PCE of 4.33% using a multilayered graphene anode.[94]

Dye-sensitized solar cells (DSSCs) are another type of OPV devices and have attracted significant interest due to their low cost and relatively high conversion efficiency (Fig. 3d). Graphene offers an attractive option as a flexible and conductive counter electrode for use in DSSCs. The counter electrode in a DSSC is essential because it injects electrons into the electrolyte and catalyzes iodine reduction after charge injection.[95] Fluorinated multilayer graphene has been used as a platinum-free counter electrode in a full DSSC and was shown to display a promising electrocatalytic activity toward triiodide reduction, with a PCE of 2.56%. A high PCE of 6.81% was obtained using a graphene nanosheet counter electrode in a DSSC.[96] Additional progress toward the development of flexible platinum-free counter electrode materials is required before such devices may reach commercialization. Lee *et al.* reported the development of a platinum-free, low-cost, flexible DSSC using a graphene film coated with a conducting polymer counter electrode (Fig. 3d).[85] The graphene–conducting polymer-based DSSCs displayed a PCE of 6.26%, comparable to the PCE of the Pt/ITO DSSC (6.68%). The high PCE was attributed to the low sheet resistance of the graphene coated with PEDOT:PSS. Fig. 3d shows the cell performances of flexible DSSCs before and after the bending tests. Very stable performances were obtained without any degradation.[85]

4.2 Light-emitting diodes

LEDs have received significant attention in academic and industrial research for applications in flashlights, traffic signals, and as light sources in video displays. LEDs are used in

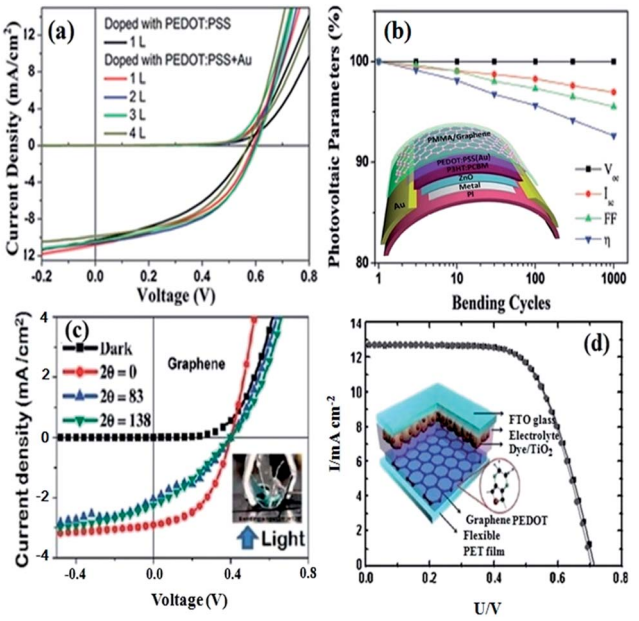

Fig. 3 (a) Current density *vs.* voltage (*J*–*V*) characteristics of OPVs with different layers of doped graphene anode. (b) Normalized photovoltaic parameters of the flexible OPVs with 2-layer CVD graphene and the inset shows the schematic diagram of an OPV with the inverted structure. (c) *J*–*V* characteristics of OPVs using CVD graphene. (d) *J*–*V* characteristics of bent and pristine DSSCs using graphene/PEDOT as the counter electrode, and the inset shows the different layers of DSSC with a graphene/PEDOT counter electrode on a flexible PET substrate. Reprinted with permission from ref. 85 & 92. Copyright 2013 WILEY-VCH Verlag GmbH & Co. KGaA, Weinheim and ref. 21 copyright 2010 American Chemical Society.

high-performance commercial displays and offer exciting colors, a high contrast ratio, and a rapid response time. LEDs are thin, lightweight, and highly energy efficient.[97] Among the various display applications in development, OLED displays are emerging as a low-cost lighting system that offers a high performance, a wide range of colors, a tunable color spectrum, good transparency, and excellent flexibility. Transparent conducting electrodes (TCEs) are an essential component of OLEDs. The development of a flexible low-cost chemically stable TCE for the production of next-generation flexible OLED-based displays would significantly advance this application area. Graphene offers an excellent option for use as a flexible TCE, as it resists degradation of the electrical properties upon bending, even at a bending radius on the millimeter length scale.[98] The primary research efforts in graphene-based TCEs for use in OLEDs[99] reported the development of a functional device prepared using a multilayer graphene electrode. The efficiency obtained was approximately 1 cd A^{-1}, lower than the efficiency obtained from a device prepared using an ITO electrode. The reduced efficiency was mainly attributed to the inefficient charge injection from the graphene electrode into the organic layer. A light-emitting electrochemical cell (LEC) device, which is similar to an OLED, was prepared using solution-processed rGO as a transparent cathode. The LEC exhibited a high quantum efficiency of 9 cd A^{-1} and a luminous efficiency of 5 lm W^{-1} at 4 V.[100] Han *et al.* described a promising method for improving the performance of flexible OLEDs by modifying the work function and sheet resistance of the graphene.[101] A photograph of a flexible OLED and a plot of the performance are shown in Fig. 4a and b. The four-layered graphene surface, with a sheet resistance of 40 Ω sq^{-1} and a transmittance of 90%, was modified by applying a conducting polymer with a gradient work function. A high current efficiency (30.2 and 98.1 cd A^{-1}) and luminous efficiency (37.2 and 107.7 lm W^{-1}) were achieved in this device. This strategy advanced the use of graphene anodes for the fabrication of high-performance flexible organic optoelectronic devices and offered a good candidate replacement material for ITO. The devices prepared using multilayer graphene, however, suffered the drawback of significant light absorption (2.3–3% per each layer). In view of this problem, Li *et al.* recently reported the preparation of a flexible OLED using monolayer graphene, which yielded a white OLED with a brightness efficiency that would be satisfactory as a general lightning source. The performance of the OLED prepared using a monolayer graphene TCE was attributed to the device structure, which permitted direct hole injection from the graphene

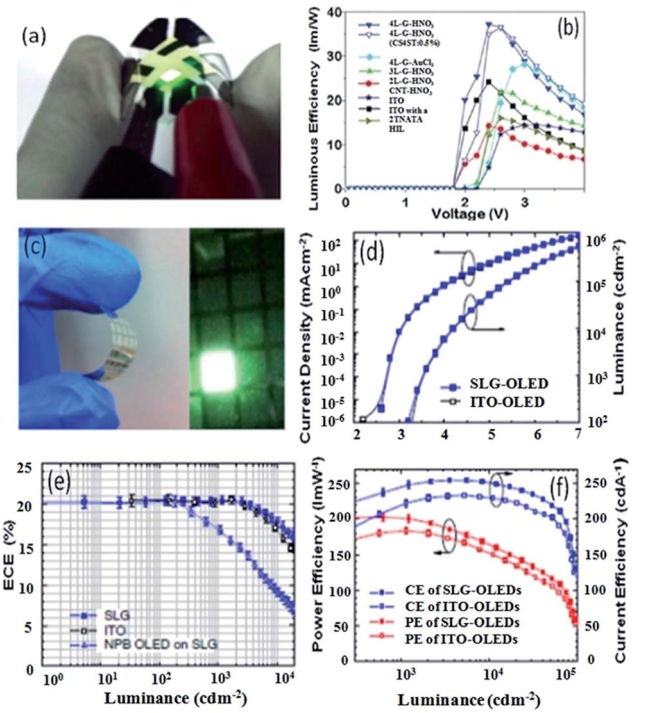

Fig. 4 (a) Phosphorescent green OLED on graphene electrodes, (b) luminous efficiency of OLED devices as various types of anode (doped graphene or ITO), (c) flexible OLEDs on single layer graphene (SLG) electrode, (d) the current density and luminance as a function of driving voltage, (e) EQE as a function of luminance for OLEDs on the SLG electrode on the flexible PET substrate, OLEDs on ITO on a glass substrate and OLEDs using the NPB hole transporting layer on SLG, and (f) PE and CE of green OLEDs on SLG and ITO with an enhanced coupling structure. The error bars represent the s.d. of multiple measurement results. Reprinted with permission from ref. 31. Copyright 2013 Macmillan Publishers Limited and ref. 101. Copyright 2012 Macmillan Publishers Limited.

electrode to the active layer, thereby reducing the carrier trapping efficiency. Fig. 4c shows a photograph of a flexible green OLED fabricated using monolayer graphene on a flexible PET substrate. The current–voltage and luminance–voltage characteristics of OLEDs prepared on either monolayer graphene or on ITO were compared and were shown to display nearly identical behaviors, with a turn-on at 2.6 V and a luminance intensity of 1000 cd m^{-2} at 4.2 V (Fig. 4d and e). These characteristics were identical because the common MoO_3 contact interface used in both devices provided a low contact and series resistance. The external quantum efficiency of the OLEDs prepared on monolayer graphene exceeded 20% with a current efficiency of 80 cd A^{-1}. The power efficiency and current efficiency of the green OLED prepared on the monolayer graphene revealed that the power efficiency and current efficiency exceeded 160 lm W^{-1} at 3000 cd m^{-2} or 250 cd A^{-1} at a high brightness of 10 000 cd m^{-2}, respectively (Fig. 4f).

4.3 Photodetectors

Graphene-based photodetectors are significant because they respond rapidly across a broad spectrum that extends from the visible to the infrared region.[104–107] Photogenerated carriers are extracted using the local potential variations near a metal–graphene interface because graphene lacks a band gap. The absorption of light induces electron–hole pair generation. The electrons and holes then separate under the external electric field induced by the photoexcitation process. There is an enhanced generation of photo carriers and a photocurrent, even in the presence of a weak internal electric field. An external voltage is applied to separate the photogenerated electron–hole pairs prior to recombination in order to improve the carrier mobilities and the photodetector response. A photoresponsivity of 8.61 A W^{-1} in a single-layer graphene limits its photoresponsivity. The absorption profile can be improved by incorporating quantum dots (QDs) onto the graphene surface. Coupling of the QDs to the π-conjugated graphene system facilitates charge injection from the excited QDs to the graphene. Charge injection proceeds faster than exciton recombination, thereby enhancing the photoresponse. A variety of QDs and inorganic nanostructures have been reported to increase the photoresponse of graphene. Mechanically exfoliated graphene decorated with PbS QDs has been reported to provide an ultrahigh photoresponsivity.[108] Similarly, Manga *et al.* prepared solution-processable PbSe–TiO_2–graphene hybrid systems for the fabrication of high-performance large-area broadband photodetectors on a PET wafer (Fig. 5a and b).[109] The incorporation of inorganic nanocrystals led to a one order of magnitude increase in the absorption coefficient. The few layer graphene (FLG)/PbSe/TiO_2 device yielded a photocurrent responsivity of 0.506 A W^{-1} and 0.13 A W^{-1} in the UV and IR regions, respectively (Fig. 5c). Electron injection occurred from the photoexcited PbSe QDs to the TiO_2 or the graphene layer, and the multicomponent assembly produced effective charge separation at the FLG/PbSe and PbSe/TiO_2 interfaces. The detectivities in the visible and IR regions were found to be $D^* \approx 3 \times 10^{13}$ Jones and $\approx 5.7 \times 10^{12}$ Jones, respectively. Peng *et al.* prepared flexible multiwalled carbon nanotube (MWCNT)/graphene hybrid materials decorated with a layered heterostructure of CdTe quantum dots (Fig. 5d). The resulting electrodes displayed an enhanced reversible photocurrent (Fig. 5e).[110] Solution-processed MWCNT/graphene films were prepared, and a flexible photoswitch was fabricated by electrostatically adsorbing an anionic CdTe layer onto the MWCNT/graphene. A high photoresponse resulted from charge transfer across the interface of the 3D layered electrodes from the CdTe excited state to the MWCNTs and graphene. The high porosity of the electrodes helped to enhance the photoresponse over 50 reversible cycles. Flexible photodetectors based on CVD-grown graphene and PbS QDs were fabricated to yield photoresponsivities of the order of 10^7 A W^{-1} with excellent bending stability (Fig. 5f and g).[111]

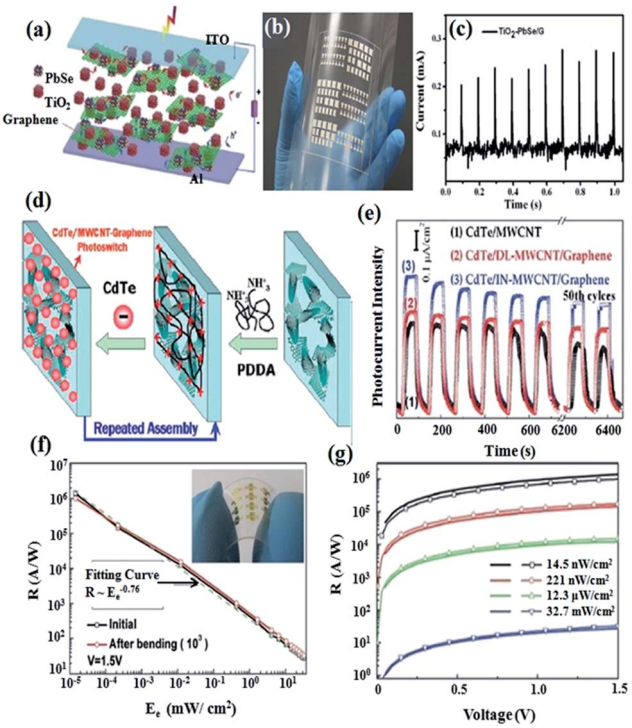

Fig. 5 (a) Schematic representation of a multiphase assembly of the FLG/PbSe/TiO_2 photodetector. (b) Large-area printed FLG/PbSe/TiO_2 photodetector patterns on a flexible substrate. (c) Photocurrent response switching measured for an FLG/PbSe/TiO_2 photodetector using a nanosecond pulsed, 1064 nm (0.5 mW cm^{-2}) laser source. (d) Schematic routes for a CdTe/MWCNT/graphene photoswitch. (e) Photoconductive ON/OFF switching charactersitics of (1) CdTe/MWCNT, (2) CdTe/DL MWCNT/graphene, and (3) CdTe/IN–MWCNT/graphene. (f) Responsivity of a photoconductor based on PbS QDs and graphene fabricated on a flexible PET substrate characterized before (solid lines) and after (dot lines) a bending test for 1000 times. (g) Responsivity of the photoconductor as functions of light irradiation characterized before and after a bending test. Reprinted with permission from ref. 109 and 111. Copyright 2012 WILEY-VCH Verlag GmbH & Co. KGaA, Weinheim and ref. 110. Copyright 2012 American Chemical Society.

Plasmonic nanostructures were used to amplify the photoresponses of graphene in graphene photodetectors.[112,113] Coupling between the plasmonic nanostructures and graphene

generated an enhanced local optical field near the graphene plane. In addition to graphene, rGO has been used to fabricate flexible photodetectors.[114] Flexible photodetectors have been fabricated from an aqueous GO solution on a PET surface based on poly(3-hexylthiophene) (P3HT). The photodetector efficiency was improved by using rGO/Au composite electrodes. Graphene nanoribbons (GNRs), which display a band gap due to quantum confinement, have been used as IR photodetectors.[115] The photoresponsivities of the GNR-based photodetectors were 1 A W^{-1} for an incident wavelength of 1550 nm at 2 V. Metal oxide nanomaterial–graphene core–shell structured photodetectors have also been reported.[116] These results indicate that graphene is a promising material for the preparation of efficient photodetectors. The performance of graphene based transparent conducting electrode and the performances of various optoelectronic devices are summarized in Table 2.

5. Conclusions

This paper has reviewed the material properties of graphene and the various synthesis and fabrication methods that have enabled the preparation of high-performance optoelectronic devices on flexible and even stretchable substrates. Recent synthesis methods have employed specialized CVD processes using low-temperature plasmas and/or roll-to-roll process lines to produce high-quality graphene in the form of large-area sheets. The new transfer printing operations include a self-release organic layer, rely on electrostatic forces, or involve electrochemical delamination to deliver the graphene sheets onto virtually any type of substrate, including lightweight flexible plastic sheets. These transfer methods can form nondestructive contacts with the underlying graphene sheets to avoid defect creation in the graphene under mechanical strain induced during the transfer process. The successful implementation of such techniques poses a significant engineering challenge, and ongoing efforts to improve the synthesis of high-quality graphene with guaranteed uniformity and reliability. The current processes would benefit from the development of defect-free transfer methods that are compatible with conventional device manufacturing processes and doping processes that can assure a stable electrical conductivity over long periods of time. Any new processes should simultaneously enable a wide range of new optoelectronic applications, such as flexible electronic OPVs, DSSCs, and OLED displays, and photosensors, as well as improve traditional rigid electronic applications based on wafer or glass substrates. These applications represent an important set of future technologies.

Acknowledgements

This work is supported by the Basic Research Program (2012R1A2A1A03006049 and 2009-0083540) through the National Research Foundation of Korea (NRF), funded by the Ministry of Science, ICT and Future Planning, and the Industrial Core Technology Development Programs, of the Korean Ministry of Knowledge Economy (grant 10033309).

References

1 S. De, T. M. Higgins, P. E. Lyons, E. M. Doherty, P. N. Nirmalraj, W. J. Blau, J. J. Boland and J. N. Coleman, *ACS Nano*, 2009, **3**, 1767.
2 Z. C. Wu, Z. H. Chen, X. Du, J. M. Logan, J. Sippel, M. Nikolou, K. Kamaras, J. R. Reynolds, D. B. Tanner, A. F. Hebard and A. G. Rinzler, *Science*, 2004, **305**, 1273.
3 M. W. Rowell, M. A. Topinka, M. D. McGehee, H. J. Prall, G. Dennler, N. S. Sariciftci, L. B. Hu and G. Gruner, *Appl. Phys. Lett.*, 2006, **88**, 233506.
4 T. M. Barnes, J. D. Bergeson, R. C. Tenent, B. A. Larsen, G. Teeter, K. M. Jones, J. L. Blackburn and J. van de Lagemaat, *Appl. Phys. Lett.*, 2010, **96**, 243309.
5 S. I. Na, S. S. Kim, J. Jo and D. Y. Kim, *Adv. Mater.*, 2008, **20**, 4061.
6 J. Ouyang, Q. F. Xu, C. W. Chu, Y. Yang, G. Li and J. Shinar, *Polymer*, 2004, **45**, 8443.
7 S. Bae, H. Kim, Y. Lee, X. F. Xu, J. S. Park, Y. Zheng, J. Balakrishnan, T. Lei, H. R. Kim, Y. I. Song, Y. J. Kim, K. S. Kim, B. Ozyilmaz, J. H. Ahn, B. H. Hong and S. Iijima, *Nat. Nanotechnol.*, 2010, **5**, 574.
8 F. Bonaccorso, Z. Sun, T. Hasan and A. C. Ferrari, *Nat. Photonics*, 2010, **4**, 611.
9 A. K. Geim and K. S. Novoselov, *Nat. Mater.*, 2007, **6**, 183.
10 K. S. Novoselov, A. K. Geim, S. V. Morozov, D. Jiang, M. I. Katsnelson, I. V. Grigorieva, S. V. Dubonos and A. A. Firsov, *Nature*, 2005, **438**, 197.
11 P. Blake, P. D. Brimicombe, R. R. Nair, T. J. Booth, D. Jiang, F. Schedin, L. A. Ponomarenko, S. V. Morozov, H. F. Gleeson, E. W. Hill, A. K. Geim and K. S. Novoselov, *Nano Lett.*, 2008, **8**, 1704.
12 R. R. Nair, P. Blake, A. N. Grigorenko, K. S. Novoselov, T. J. Booth, T. Stauber, N. M. R. Peres and A. K. Geim, *Science*, 2008, **320**, 1308.
13 X. Wang, L. J. Zhi and K. Mullen, *Nano Lett.*, 2008, **8**, 323.
14 C. Lee, X. Wei, J. W. Kysar and J. Hone, *Science*, 2008, **321**, 385.
15 S. Pang, H. N. Tsao, X. L. Feng and K. Mullen, *Adv. Mater.*, 2009, **21**, 3488.
16 C. A. Di, D. C. Wei, G. Yu, Y. Q. Liu, Y. L. Guo and D. B. Zhu, *Adv. Mater.*, 2008, **20**, 3289.
17 W. Liu, B. L. Jackson, J. Zhu, C. Q. Miao, C. H. Chung, Y. J. Park, K. Sun, J. Woo and Y. H. Xie, *ACS Nano*, 2010, **4**, 3927.
18 V. C. Tung, M. J. Allen, Y. Yang and R. B. Kaner, *Nat. Nanotechnol.*, 2009, **4**, 25.
19 L. Liao, Y. C. Lin, M. Bao, R. Cheng, J. Bai, Y. Liu, Y. Qu, K. L. Wang, Y. Huang and X. Duan, *Nature*, 2010, **467**, 305.
20 T. J. Echtermeyer, M. C. Lemme, M. Baus, B. N. Szafranek, A. K. Geim and H. Kurz, *IEEE Electron Device Lett.*, 2008, **29**, 952.
21 L. G. De Arco, Y. Zhang, C. W. Schlenker, K. Ryu, M. E. Thompson and C. W. Zhou, *ACS Nano*, 2010, **4**, 2865.
22 Q. Su, S. P. Pang, V. Alijani, C. Li, X. L. Feng and K. Mullen, *Adv. Mater.*, 2009, **21**, 3191.

23 X. Wang, L. J. Zhi, N. Tsao, Z. Tomovic, J. L. Li and K. Mullen, *Angew. Chem., Int. Ed.*, 2008, **47**, 2990.
24 A. Konar, T. Fang and D. Jena, *Phys. Rev. B: Condens. Matter Mater. Phys.*, 2010, **82**, 115452.
25 S. Some, J. Kim, K. Lee, A. Kulkarni, Y. Yoon, S. Lee, T. Kim and H. Lee, *Adv. Mater.*, 2012, **24**, 5481.
26 M. W. Lin, C. Ling, Y. Zhang, H. J. Yoon, M. M. C. Cheng, L. A. Agapito, N. Kioussis, N. Widjaja and Z. Zhou, *Nanotechnology*, 2011, **22**, 265201.
27 P. Peumans, A. Yakimov and S. R. Forrest, *J. Appl. Phys.*, 2003, **93**, 3693.
28 A. Andersson, N. Johansson, P. Bröms, N. Yu, D. Lupo and W. R. Salaneck, *Adv. Mater.*, 1998, **10**, 859.
29 A. Kumar and C. Zhou, *ACS Nano*, 2010, **4**, 11.
30 K. S. Novoselov, V. I. Fal'ko, L. Colombo, P. R. Gellert, M. G. Schwab and K. Kim, *Nature*, 2012, **490**, 192.
31 N. Li, S. Oida, G. S. Tulevski, S. J. Han, J. B. Hannon, D. K. Sadana and T. C. Chen, *Nat. Commun.*, 2013, **4**, 2294.
32 K. S. Novoselov, A. K. Geim, S. V. Morozov, D. Jiang, Y. Zhang, S. V. Dubonos, I. V. Grigorieva and A. A. Firsov, *Science*, 2004, **306**, 666.
33 K. S. Kim, Y. Zhao, H. Jang, S. Y. Lee, J. M. Kim, K. S. Kim, J. H. Ahn, P. Kim, J. Y. Choi and B. H. Hong, *Nature*, 2009, **457**, 706.
34 Y. Lee, S. Bae, H. Jang, S. Jang, S. E. Zhu, S. H. Sim, Y. I. Song, B. H. Hong and J. H. Ahn, *Nano Lett.*, 2010, **10**, 490.
35 S. Y. Kwon, C. V. Ciobanu, V. Petrova, V. B. Shenoy, J. Bareño, V. Gambin, I. Petrov and S. Kodambaka, *Nano Lett.*, 2009, **9**, 3985.
36 M. Eizenberg and J. M. Blakely, *Surf. Sci.*, 1979, **82**, 228.
37 Q. Yu, J. Lian, S. Siriponglert, H. Li, Y. P. Chen and S. S. Pei, *Appl. Phys. Lett.*, 2008, **93**, 113103.
38 A. Reina, X. Jia, J. Ho, D. Nezich, H. Son, V. Bulovic, M. S. Dresselhaus and J. Kong, *Nano Lett.*, 2009, **9**, 30.
39 X. Li, W. Cai, J. An, S. Kim, J. Nah, D. Yang, R. Piner, A. Velamakanni, I. Jung, E. Tutuc, S. K. Banerjee, L. Colombo and R. S. Ruoff, *Science*, 2009, **324**, 1312.
40 X. Li, Y. Zhu, W. Cai, M. Borysiak, B. Han, D. Chen, R. D. Piner, L. Colombo and R. S. Ruoff, *Nano Lett.*, 2009, **9**, 4359.
41 T. Kobayashi, M. Bando, N. Kimura, K. Shimizu, K. Kadono, N. Umezu, K. Miyahara, S. Hayazaki, S. Nagai, Y. Mizuguchi, Y. Murakami and D. Hobara, *Appl. Phys. Lett.*, 2013, **102**, 023112.
42 J. Kim, M. Ishihara, Y. Koga, K. Tsugawa, M. Hasegawa and S. Iijima, *Appl. Phys. Lett.*, 2011, **98**, 091502.
43 Y.-J. Kim, S. J. Kim, M. H. Jung, K. Y. Choi, S. Bae, S.-K. Lee, Y. Lee, D. Shin, B. Lee, H. Shin, M. Choi, K. Park, J.-H. Ahn and B. H. Hong, *Nanotechnology*, 2012, **23**, 344016.
44 G. D. Yuan, W. J. Zhang, Y. Yang, Y. B. Tang, Y. Q. Li, J. X. Wang, X. M. Meng, Z. B. He, C. M. L. Wu, I. Bello, C. S. Lee and S. T. Lee, *Chem. Phys. Lett.*, 2009, **467**, 361.
45 K. J. Peng, C. L. Wu, Y. H. Lin, Y. J. Liu, D. P. Tsai, Y. H. Pai and G. R. Lin, *J. Mater. Chem. C*, 2013, **1**, 3862.
46 B. C. Brodie, *Philos. Trans. R. Soc. London*, 1959, **149**, 249.
47 S. Stankovich, D. A. Dikin, R. D. Piner, K. A. Kohlhaas, A. Kleinhammes, Y. Jia, Y. Wu, S. T. Nguyen and R. S. Ruoff, *Carbon*, 2007, **45**, 1558.
48 S. Stankovich, R. D. Piner, X. Chen, N. Wu, S. T. Nguyen and R. S. Ruoff, *J. Mater. Chem.*, 2006, **16**, 155.
49 V. C. Tung, M. J. Allen, Y. Yang and R. B. Kaner, *Nat. Nanotechnol.*, 2009, **4**, 25.
50 C. Gomez-Navarro, R. T. Weitz, A. M. Bittner, M. Scolari, A. Mews, M. Burghard and K. Kern, *Nano Lett.*, 2007, **7**, 3499.
51 D. A. Sokolov, K. R. Shepperd and T. M. Orlando, *J.Phys. Chem. Lett.*, 2010, **1**, 2633.
52 S. Guo and S. Dong, *Chem. Soc. Rev.*, 2011, **40**, 2644.
53 H. A. Becerril, J. Mao, Z. Liu, R. M. Stoltenberg, Z. Bao and Y. Chen, *ACS Nano*, 2008, **2**, 463.
54 K. Parvez, R. Li, S. R. Puniredd, Y. Hernandez, F. Hinkel, S. Wang, X. Feng and K. Mullen, *ACS Nano*, 2013, **7**, 3598.
55 D. Li, M. B. Muller, S. Gilje, R. B. Kaner and G. G. Wallace, *Nat. Nanotechnol.*, 2008, **3**, 101.
56 H. Chen, M. B. Muller, K. J. Gilmore, G. G. Wallace and D. Li, *Adv. Mater.*, 2008, **20**, 3557.
57 S. Stankovich, D. A. Dikin, G. H. B. Dommett, K. M. Kohlhaas, E. J. Zimney, E. A. Stach, R. D. Piner, S. T. Nguyen and R. S. Ruoff, *Nature*, 2006, **442**, 282.
58 Y. Zhang, T. T. Tang, C. Girit, Z. Hao, M. C. Martin, A. Zettl, M. F. Crommie, Y. R. Shen and F. Wang, *Nature*, 2009, **459**, 820.
59 C. Yan, K. S. Kim, S. K. Lee, S. H. Bae, B. H. Hong, J. H. Kim, H. J. Lee and J. H. Ahn, *ACS Nano*, 2011, **6**, 2096.
60 G. X. Ni, Y. Zheng, S. Bae, C. Y. Tan, O. Kahya, J. Wu, B. H. Hong, K. Yao and B. Özyilmaz, *ACS Nano*, 2012, **6**, 3935.
61 J. H. Chen, C. Jang, S. D. Xiao, M. Ishigami and M. S. Fuhrer, *Nat. Nanotechnol.*, 2008, **3**, 206.
62 K. K. Kim, A. Reina, Y. Shi, H. Park, L. J. Li, Y. H. Lee and J. Kong, *Nanotechnology*, 2010, **21**, 285205.
63 S. Park and R. S. Ruoff, *Nat. Nanotechnol.*, 2009, **4**, 217.
64 L. J. Cote, F. Kim and J. X. Huang, *J. Am. Chem. Soc.*, 2009, **131**, 1043.
65 X. L. Li, G. Y. Zhang, X. D. Bai, X. M. Sun, X. R. Wang, E. Wang and H. J. Dai, *Nat. Nanotechnol.*, 2008, **3**, 538.
66 X. Lin, J. Jia, N. Yousefi, X. Shen and J.-K. Kim, *J. Mater. Chem. C*, 2013, **1**, 6869.
67 S.-K. Lee, H. Y. Jang, S. Jang, E. Choi, B. H. Hong, J. Lee, S. Park and J.-H. Ahn, *Nano Lett.*, 2012, **12**, 3472.
68 X. Liang, B. A. Sperling, I. Calizo, G. Cheng, C. A. Hacker, Q. Zhang, Y. Obeng, K. Yan, H. Peng, Q. Li, X. Zhu, H. Yuan, A. R. H. Walker, Z. Liu, L. Peng and C. A. Richter, *ACS Nano*, 2011, **5**, 9144.
69 J. Song, F. Y. Kam, R. Q. Png, W. L. Seah, J. M. Zhuo, G. K. Lim, P. K. H. Ho and L. L. Chua, *Nat. Nanotechnol.*, 2013, **8**, 356.
70 E. H. Lock, M. Baraket, M. Laskoski, S. P. Mulvaney, W. K. Lee, P. E. Sheehan, D. R. Hines, J. T. Robinson, J. Tosado, M. S. Fuhrer, S. C. Hernandez and S. G. Walton, *Nano Lett.*, 2011, **12**, 102.

71 T. Yoon, W. C. Shin, T. Y. Kim, J. H. Mun, T. Kim and B. J. Cho, *Nano Lett.*, 2012, **12**, 1448.
72 D. Y. Wang, I. S. Huang, P. H. Ho, S. S. Li, Y. C. Yeh, D. W. Wang, W. L. Chen, Y. Y. Lee, Y. M. Chang, C. C. Chen, C. T. Liang and C. W. Chen, *Adv. Mater.*, 2013, **25**, 4521.
73 L. Gao, W. Ren, H. Xu, L. Jin, Z. Wang, T. Ma, L. P. Ma, Z. Zhang, Q. Fu, L. M. Peng, X. Bao and H. M. Cheng, *Nat. Commun.*, 2012, **3**, 699.
74 G. Eda and M. Chhowalla, *Adv. Mater.*, 2010, **22**, 2392.
75 F. Kim, L. J. Cote and J. Huang, *Adv. Mater.*, 2010, **22**, 1954.
76 J. X. Geng, L. J. Liu, S. B. Yang, S. C. Youn, D. W. Kim, J. S. Lee, J. K. Choi and H. T. Jung, *J. Phys. Chem. C*, 2010, **114**, 14433.
77 S. Li, Y. Luo, W. Li, W. Yu, S. Wu, P. Hou, Q. Yang, Q. Meng, C. Liu and H. M. Cheng, *Adv. Energy Mater.*, 2011, **1**, 486.
78 L. Hu, D. S. Hecht and G. Gruner, *Nano Lett.*, 2004, **4**, 2513.
79 Q. Zheng, L. Shi, P.-C. Ma, Q. Xue, J. Li, Z. Tang and J. Yang, *RSC Adv.*, 2013, **3**, 4680.
80 Q. Zheng, W. H. Ip, X. Lin, N. Yousefi, K. K. Yeung, Z. Li and J.-K. Kim, *ACS Nano*, 2010, **5**, 6039.
81 X. Wan, G. Long, L. Huang and Y. Chen, *Adv. Mater.*, 2011, **23**, 5342.
82 D. Jariwal, V. K. Sangwan, L. J. Lauhon, T. J. Marksab and M. C. Hersam, *Chem. Soc. Rev.*, 2013, **42**, 2824.
83 X. Huang, Z. Zeng, Z. Fan, J. Liu and H. Zhang, *Adv. Mater.*, 2012, **24**, 5979.
84 Z. Liu, J. Li, Z. H. Sun, G. Tai, S. P. Lau and F. Yan, *ACS Nano*, 2012, **6**, 810.
85 K. S. Lee, Y. Lee, J. Y. Lee, J.-H. Ahn and J. H. Park, *ChemSusChem*, 2012, **5**, 379.
86 Z. Yin, J. Zhu, Q. He, X. Cao, C. Tan, H. Chen, Q. Yan and H. Zhang, *Adv. Energy Mater.*, 2014, **4**, 1300574.
87 Z. Liu, Q. Liu, Y. Huang, Y. Ma, S. Yin, X. Zhang, W. Sun and Y. Chen, *Adv. Mater.*, 2008, **20**, 3924.
88 N. Yang, J. Zhai, D. Wang, Y. Chen and L. Jiang, *ACS Nano*, 2010, **4**, 887.
89 Y. Xu, G. Long, L. Huang, Y. Huang, X. Wan, Y. Ma and Y. Chen, *Carbon*, 2010, **48**, 3308.
90 V. C. Tung, L. M. Chen, M. J. Allen, J. K. Wassei, K. Nelson, R. B. Kaner and Y. Yang, *Nano Lett.*, 2009, **9**, 1949.
91 E. Kymakis, K. Savva, M. M. Stylianakis, C. Fotakis and E. Stratakis, *Adv. Funct. Mater.*, 2013, **23**, 2742.
92 Z. Liu, J. Li and F. Yan, *Adv. Mater.*, 2013, **25**, 4296.
93 S. Lee, J. S. Yeo, Y. Ji, C. Cho, D. Y. Kim, S. I. Na, B. H. Lee and T. Lee, *Nanotechnology*, 2012, **23**, 344013.
94 H. Kim, S. H. Bae, T. H. Han, K. G. Lim, J.-H. Ahn and T. W. Lee, *Nanotechnology*, 2014, **25**, 014012.
95 S. Das, P. Sudhagar, V. Verma, D. Song, E. Ito, S. Y. Lee, Y. S. Kang and W. B. Choi, *Adv. Funct. Mater.*, 2011, **21**, 3729.
96 D. W. Zhang, X. D. Li, H. B. Li, S. Chen, Z. Sun, X. J. Yin and S. M. Huang, *Carbon*, 2011, **49**, 5382.
97 B. W. D'Andrade, R. J. Holmes and S. R. Forrest, *Adv. Mater.*, 2004, **16**, 624.
98 S. Reineke, F. Lindner, G. Schwartz, N. Seidler, K. Walzer, B. Lüssem and K. Leo, *Nature*, 2009, **459**, 234.
99 J. Wu, M. Agrawal, H. A. Becerril, Z. Bao, Z. Liu, Y. Chen and P. Peumans, *ACS Nano*, 2010, **4**, 43.
100 P. Matyba, H. Yamaguchi, G. Eda, M. Chhowalla, L. Edman and N. D. Robinson, *ACS Nano*, 2010, **4**, 637.
101 T. H. Han, Y. Lee, M. R. Choi, S. H. Woo, S. H. Bae, B. H. Hong, J.-H. Ahn and T. W. Lee, *Nat. Photonics*, 2012, **6**, 105.
102 G. Zhu, L. Pan, T. Lu, T. Xu and Z. J. Sun, *Mater. Chem.*, 2011, **21**, 14869.
103 T. Sun, Z. Wang, Z. Shi, G. Ran, W. Xu, Z. Wang, Y. Li, L. Dai and G. Qin, *Appl. Phys. Lett.*, 2010, **96**, 13330.
104 F. N. Xia, T. Mueller, Y. M. Lin, A. Valdes-Garcia and P. Avouris, *Nat. Nanotechnol.*, 2009, **4**, 839.
105 T. Mueller, F. N. Xia and P. Avouris, *Nat. Photonics*, 2010, **4**, 297.
106 A. Urich, K. Unterrainer and T. Mueller, *Nano Lett.*, 2011, **11**, 2804.
107 Y. Zhang, T. Liu, B. Meng, X. Li, G. Liang, X. Hu and Q. J. Wang, *Nat. Commun.*, 2013, **4**, 1811.
108 G. Konstantatos, M. Badioli, L. Gaudreau, J. Osmond, M. Bernechea, F. P. G. de Arquer, F. Gatti and F. H. L. Koppens, *Nat. Nanotechnol.*, 2012, **7**, 363.
109 K. K. Manga, J. Wang, M. Lin, J. Zhang, M. Nesladek, V. Nalla, W. Ji and K. P. Loh, *Adv. Mater.*, 2012, **24**, 1697.
110 L. Peng, Y. Feng, P. Lv, D. Lei, Y. Shen, Y. Li and W. Feng, *J. Phys. Chem. C*, 2012, **116**, 4970.
111 Z. Sun, Z. Liu, J. Li, G. Tai, S. Lau and F. Yan, *Adv. Mater.*, 2012, **24**, 5878.
112 T. J. Echtermeyer, L. Britnell, P. K. Jasnos, A. Lombardo, R. V. Gorbachev, A. N. Grigorenko, A. K. Geim, A. C. Ferrari and K. S. Novoselov, *Nat. Commun.*, 2011, **2**, 458.
113 Y. Liu, R. Cheng, L. Liao, H. Zhou, J. Bai, G. Liu, L. Liu, Y. Huang and X. Duan, *Nat. Commun.*, 2011, **2**, 579.
114 Y. Guo, B. Wu, H. Liu, Y. Ma, Y. Yang, J. Zheng, G. Yu and Y. Liu, *Adv. Mater.*, 2011, **23**, 4626.
115 B. Chitara, L. S. Panchakarla, S. B. Krupanidhi and C. N. R. Rao, *Adv. Mater.*, 2011, **23**, 5419.
116 D. Shao, M. Yu, H. Sun, T. Hu, J. Lian and S. Sawyer, *Nanoscale*, 2013, **5**, 3664.

